

## PHYSICAL PROPERTIES OF RF-SPUTTERED ZnSe THIN FILMS FOR PHOTOVOLTAIC APPLICATIONS: INFLUENCE OF FILM THICKNESS

L. ION<sup>1</sup>, S. IFTIMIE<sup>1</sup>, A. RADU<sup>1</sup>, V.A. ANTOHE<sup>1,2</sup>, O. TOMA<sup>1</sup>, S. ANTOHE<sup>1,3</sup>

<sup>1</sup> University of Bucharest, Faculty of Physics, 405 Atomistilor Street, 077125 Măgurele, Ilfov, Romania  
<sup>2</sup> Université catholique de Louvain (UCLouvain), Institute of Condensed Matter and Nanosciences (IMCN),  
Place Croix du Sud 1, B-1348 Louvain-la-Neuve, Belgium

<sup>3</sup> Academy of Romanian Scientists, 3 Ilfov Street, 050045 Bucharest, Romania

Corresponding author: Stefan ANTOHE, E-mail: [santohe@solid.fizica.unibuc.ro](mailto:santohe@solid.fizica.unibuc.ro)

**Abstract.** Zinc selenide (ZnSe) thin films were deposited by radio frequency magnetron sputtering onto optical glass (for structural, morphological and optical characterizations) and onto indium-tin-oxide (ITO) coated glass substrates, to be used for producing photovoltaic structures based on zinc selenide/cadmium telluride (CdTe) thin film heterojunctions. The crystalline structure of ZnSe thin films was investigated by X-ray diffraction; the films are polycrystalline with a marked (111) texture. The structure of the films deposited on glass and on ITO covered glass is analyzed comparatively. Surface morphology parameters of the films were determined by atomic force microscopy. Spectroscopic ellipsometry and optical absorption spectroscopy measurements were used to characterize the optical properties of ZnSe films. Experimentally determined band gap values were 2.83 – 2.84 eV. The temperature dependence of the electrical resistivity was investigated from room temperature down to 10 K. ITO/ZnSe/CdTe structures in superstrate configuration were produced by depositing the absorber CdTe layer by thermal vacuum evaporation (TVE). Action spectra of the external quantum efficiency (EQE) of the structures were measured before and after irradiation with protons (3 MeV), and the effect of irradiation is discussed.

**Key words:** ZnSe films, ZnSe/CdTe heterojunctions, rf-magnetron sputtering, photovoltaic effect.

### 1. INTRODUCTION

A<sup>II</sup>B<sup>VI</sup> binary semiconducting compounds are of great scientific and technological interest due to their applications in electronic and optoelectronic devices. Among them, zinc selenide (ZnSe) is particularly interesting for applications related to the interaction with infrared and visible light. Having good mechanical and chemical properties, ZnSe thin films are suitable candidates for semiconductor window layers in the architecture of photovoltaic cells. ZnSe has a large direct band gap of 2.67 eV at room temperature, high optical transmittance over a large spectral range between 0.6 – 20 μm and good photosensitivity. Optoelectronic devices based on ZnSe thin films were produced and characterized, such as light emitting diodes [1, 2], solar cells [3, 4, 5, 6], photo detectors [7], transistors [8], dielectric mirrors [9], etc. In thin film based solar cells technology, ZnSe is a less toxic alternative to the widely used cadmium sulfide (CdS); it may be used as window layer in CuInGaSe<sub>2</sub> and CdTe-based solar cells [10, 11, 12, 13, 14, 15, 16]. Various techniques were used for deposition of ZnSe thin films: chemical bath deposition [17, 18, 19], thermal evaporation (TVE) [20, 21, 22], chemical vapor deposition [6], molecular beam epitaxy [23] or electrodeposition [24]. We choose to deposit ZnSe thin films by rf-magnetron sputtering due to the excellent control of film thickness uniformity proved by this deposition method [25, 26, 27]. The effect of film thickness on structural, morphological, electrical, and optical properties of sputtered ZnSe thin films deposited on optical glass was investigated, in view of their use in thin film based solar cells. This paper is organized as follows: first the results of a study on structural, morphological, electrical, and optical properties of ZnSe thin films deposited by rf-magnetron sputtering are presented. Next, we report the results of a study on the photovoltaic response of a structure based on ZnSe/CdTe heterojunction and we describe how this response is influenced by irradiation with 3 MeV protons. With protons representing the main components of cosmic rays, such a study is relevant in view of possible applications of this type of photovoltaic structures in space technology.

## 2. EXPERIMENTAL DETAILS

Thin films of ZnSe were deposited by rf-magnetron sputtering on optical glass (Corning) substrate, for material characterization. Before deposition, the substrates were ultrasonically cleaned in acetone for 10 min. The deposition chamber was first evacuated to  $10^{-3}$  Pa, before admission of Ar gas up to the working pressure of 0.86 Pa. The target-to-substrate distance was set to 80 mm, the power applied to the magnetron was 90 W and the substrate temperature was set to 220°C during deposition. Films with thickness of 110 nm, 150 nm and 175 nm were deposited.

ZnSe/CdTe heterojunctions in superstrate configuration were produced by depositing ZnSe films in the same conditions on optical glass coated with 35 nm indium tin oxide (ITO) layers (used as front contacts); the sheet resistance of ITO layers was 12  $\Omega$ /sq. CdTe absorber layers were subsequently deposited by TVE, this method being proved to be suitable in obtaining CdTe films with good crystallinity [30]. Cadmium telluride powder (Aldrich, 99.99% purity) was sublimated, in a chamber evacuated prior to deposition to  $4 \times 10^{-2}$  Pa, at 750°C, onto the glass/ITO/ZnSe structure maintained at 270°C during deposition. The thickness of CdTe layer was 3  $\mu$ m in the case of all structures. After deposition of CdTe layers, the structures were annealed at 300°C *in-situ* for 10 min. This post-deposition treatment was performed to improve the structural and chemical quality of the films. Next, treatments in CdCl<sub>2</sub> vapors were performed on the structure glass/ITO/ZnSe/CdTe in order to improve their photovoltaic response [31, 32, 33]. CdCl<sub>2</sub> powder (Aldrich) was sublimated *in vacuo* from a quartz crucible heated at 250°C, while the temperature of the heterostructures was maintained at 100°C. Photovoltaic cells were completed by depositing the back contacts (a 50 nm copper layer followed by a 90 nm gold layer) by TVE. During this procedure, the structures were maintained at 170°C; after the deposition of Cu:Au back electrodes, the entire cell was annealed at 200°C for 10 min.

Structural properties of ZnSe thin films deposited by rf-magnetron sputtering were investigated by X-ray diffraction (XRD) using a Bruker D8 Discover diffractometer with Cu<sub>K $\alpha$ 1</sub> radiation ( $\lambda=1.5406$  Å). Morphological investigations were performed by atomic force microscopy (AFM), in contact mode.

The electrical resistivity of the films was measured using Van der Pauw method, in a temperature range of 300 K – 10 K. The samples were introduced in an evacuated He closed cycle cryostat, the experimental setup including a Keithley 6517a electrometer, a Keithley 2400 SourceMeter and a Lakeshore 332 temperature controller, controlled by PC.

Optical properties were investigated by spectroscopic ellipsometry (SE), using a spectro-ellipsometer Woollam WVASE 32 (spectral range available was between 250 nm up to 1.7  $\mu$ m) and by absorption spectroscopy, using a double beam Perkin Elmer Lambda 35 spectrometer. Action spectra of ITO/ZnSe/CdTe/Cu:Au structures were measured by using a setup including a monochromator, a Keithley 2400 SourceMeter and a Newport Oriel solar simulator, controlled by a PC. Experiments related to the effects induced by irradiation with protons (3 MeV, fluencies of  $10^{13}$  cm<sup>-2</sup>) on the photovoltaic response of ITO/ZnSe/CdTe/Cu:Au devices were performed; proton beams were produced by using a 3 MV Tandemron accelerator [34].

## 3. RESULTS AND DISCUSSION

### 3.1. ZnSe films

Grazing incidence X-ray diffraction (GIXRD) spectra recorded for ZnSe films deposited on optical glass and optical glass covered with ITO are shown in Figure 1. This experimental geometry is well suited for thin films, as the optical path of X-ray photons is increased in the film and the scattering volume is kept constant over the entire  $2\theta$  scanned range. For quantitative determinations, the region corresponding to the most intense diffraction peak, (111), was scanned in Bragg-Brentano theta-theta geometry, with the step size  $\Delta\theta = 0.005^\circ$ . The structure of the spectra is similar for both types of substrates used here; ZnSe films are polycrystalline, containing the thermodynamically stable cubic phase (PDF2 37-1463). All the films show a (111) texture. For ZnSe films deposited on ITO covered optical glass, supplementary peaks corresponding to ITO substrates are observed (Fig. 1, right side).

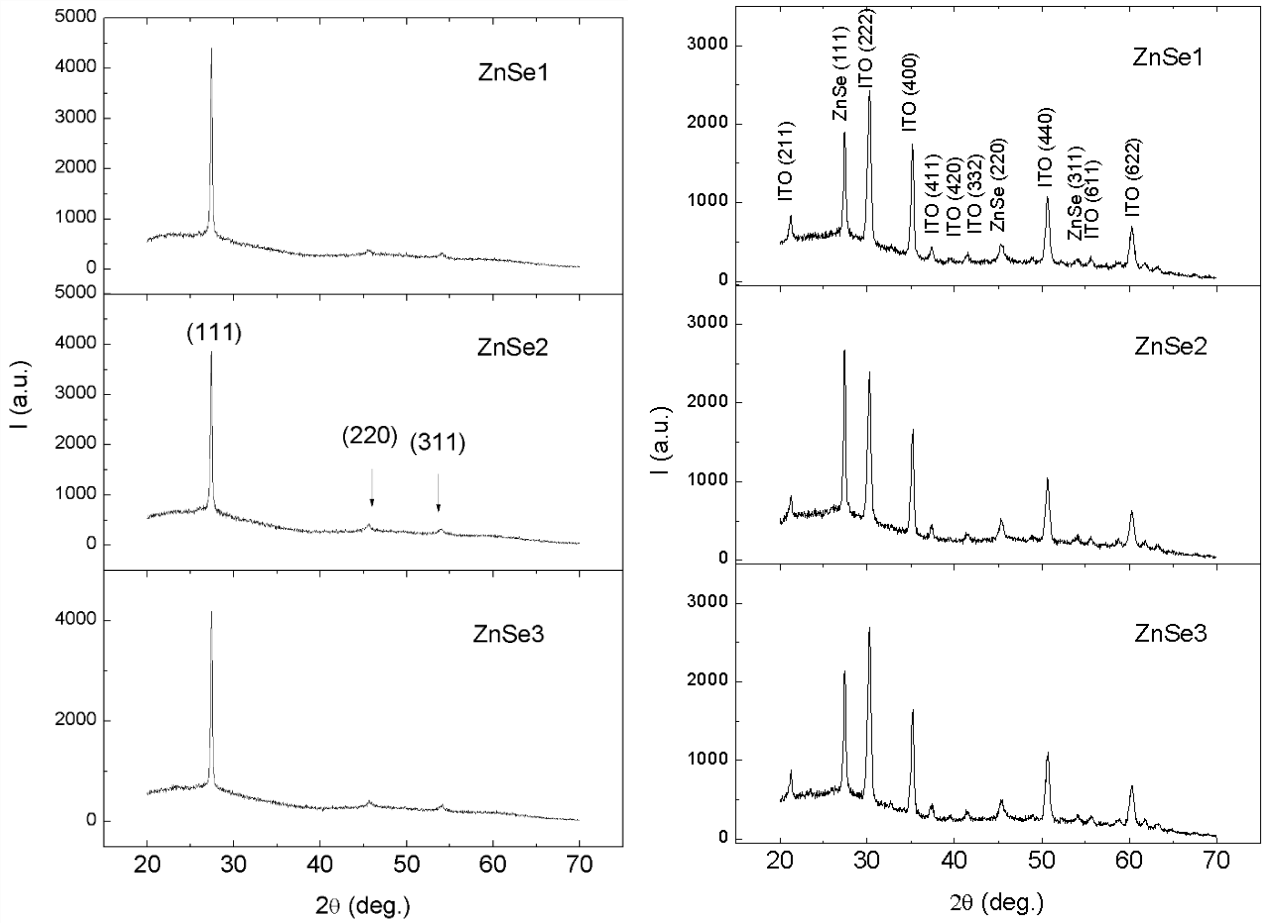


Fig. 1 – GIXRD spectra recorded for ZnSe films deposited on optical glass (left side) and optical glass covered with ITO (right side). ZnSe1, ZnSe2 and ZnSe3 indicate the films with 110 nm, 150 nm and 175 nm thickness, respectively.

High influx of adsorbed atoms and high growth rate are typical for deposition by plasma assisted techniques. That leads to incorporation of defects in the structure of the films and stoichiometry variations in the growth surface associated with these defects have an impact on the surface energy, facilitating the stabilization of (111) surface (the surface of minimum energy is (110) in the case of cubic structure of ZnSe [35]). This could explain the presence of (311) peaks, orientation which makes a small angle with the (111) orientation. The most prominent (111) diffraction peak of ZnSe was scanned in Bragg-Brentano theta-theta geometry and experimental results were fit analytically using Voigt profiles (the red line in Fig. 2). After correcting for instrumental broadening, integral breadths  $\beta_G$  and  $\beta_L$  of Gauss and Lorentz components of Voigt profile were used to extract the crystalline coherence length  $D_{ef}$  for (111) orientation and the micro-strain,  $\langle \varepsilon^2 \rangle^{1/2}$ , induced by mechanical stresses developed during growth, by using [36]:

$$D_{ef} = \frac{0.9\lambda}{\beta_L \cos \theta}, \quad (1)$$

$$\beta_G = 2\sqrt{2\pi} \langle \varepsilon^2 \rangle^{1/2} \tan \theta. \quad (2)$$

The results are collected in Table 1. Both microscopic and macroscopic mechanical stresses (the last one characterized by the average strain  $\frac{\Delta a}{a_0}$  with  $a_0 = 5.669 \text{ \AA}$ , the ideal ZnSe lattice constant, according to PDF2 37-1463) are small and practically do not depend on the thickness of studied ZnSe samples. Crystallite sizes have a tendency to increase with film thickness.

*Table 1*  
Structural parameters of fabricated ZnSe thin films

Sample	Thickness (nm)	$2\theta_0$ (deg.)	$a$ (Å)	$D_{ef}$ (nm)	$\langle \epsilon^2 \rangle^{1/2}$	$\frac{\Delta a}{a_0}$
ZnSe/glass	110	27.41	5.63	54.3	$1.97 \times 10^{-3}$	$6.35 \times 10^{-3}$
ZnSe/ITO/glass	110	27.43	5.63	43.1	$2.41 \times 10^{-3}$	$6.35 \times 10^{-3}$
ZnSe/glass	150	27.38	5.64	76.2	$2.80 \times 10^{-3}$	$5.29 \times 10^{-3}$
ZnSe/ITO/glass	150	27.41	5.63	38.2	$1.75 \times 10^{-3}$	$6.35 \times 10^{-3}$
ZnSe/glass	175	27.41	5.63	78.4	$2.85 \times 10^{-3}$	$6.35 \times 10^{-3}$
ZnSe/ITO/glass	175	27.43	5.62	81.5	$3.07 \times 10^{-3}$	$7.06 \times 10^{-3}$

The morphology of the surface of the films was characterized by atomic force microscopy (AFM, Fig. 3) and characteristic parameters extracted from AFM scans (surface roughness and statistical parameters of grains distributions on film surfaces) are shown in Table 2. Relatively smooth surfaces were observed, without drops formed during sputtering. Thicker ZnSe films have more symmetric distributions of grain heights over investigated surfaces and smaller roughness values.

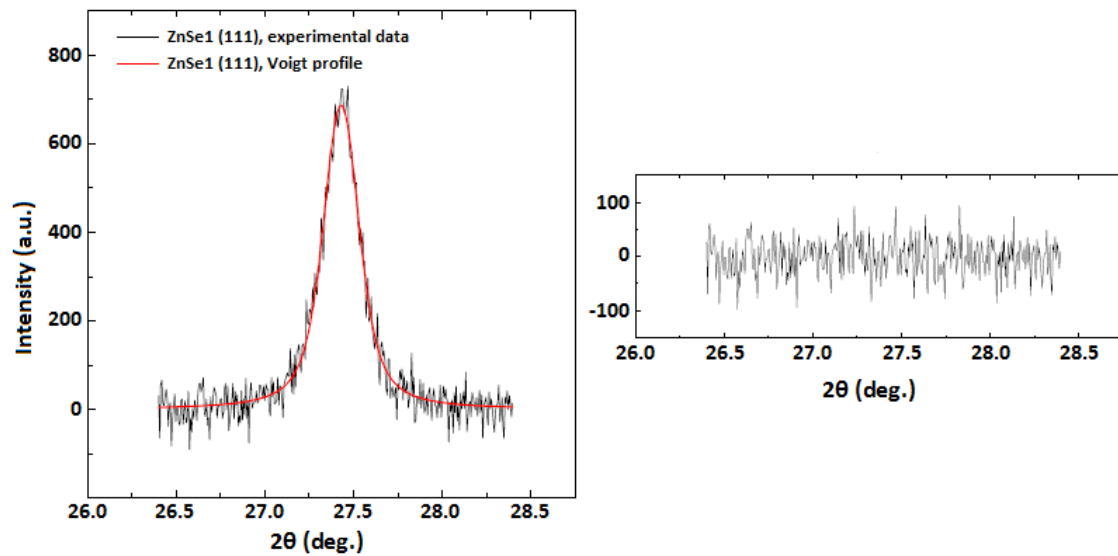


Fig. 2 – (111) diffraction peak of the ZnSe film (110 nm thick), recorded in Bragg-Brentano theta-theta geometry (black line) and the Voigt profile obtained by fit (red line). The residuals of the fit procedure are also shown.

*Table 2*

Parameters characterizing the surface morphology of ZnSe films sputtered on optical glass, as extracted from AFM scans, and optical band gap values

Sample	Thickness (nm)	RMS roughness (nm)	Skewness parameter	Kurtosis parameters	$E_g$ (eV)
ZnSe/glass	110	3.1	0.56	2.95	2.84
ZnSe/glass	150	2.4	0.38	2.41	2.83
ZnSe/glass	175	2.1	0.26	2.13	2.83

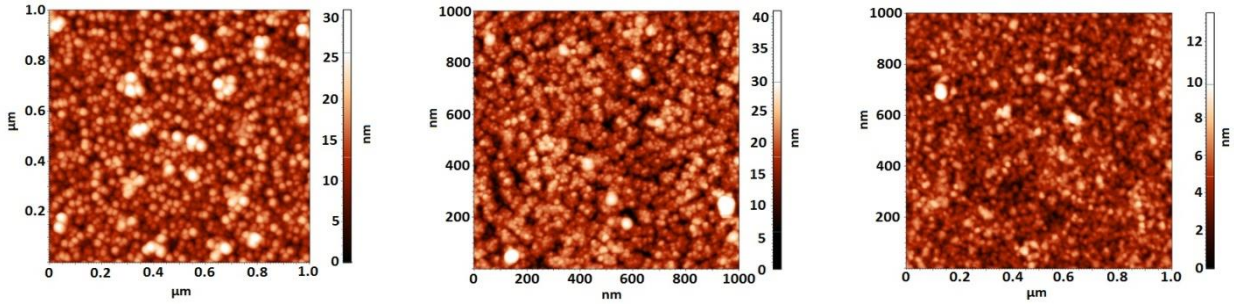


Fig. 3 – AFM images for ZnSe films sputtered on optical glass; samples with thickness of 110 nm (left), 150 nm (center) and 175 nm (right) are shown.

Optical properties of the films were investigated by absorption spectroscopy and spectroscopic ellipsometry. The dependence of the absorption coefficient,  $\alpha$  on the energy of incident photons near the fundamental absorption edge, in semiconductors with direct absorption edge (ZnSe belongs to this class of semiconductors), is given by:

$$\alpha(\hbar\omega) = \alpha_0 \frac{(\hbar\omega - E_g)^{1/2}}{\hbar\omega}, \quad (3)$$

in which  $E_g$  is the direct band gap. Equation (3), describing direct allowed transitions, was used to determine the band gap of the films, shown in Table 2 (see Fig. 4). Optical band gaps of the films are larger than the band gap of ZnSe bulk crystal (2.67 eV), due to the quantum confinement of electronic states in a smaller volume inside the crystallites. The quantum confinement explains also the observed trend of the absorption coefficient, which increases with decreasing film thickness due to a better overlap of the wavefunctions, associated to valence band and conduction band states, resulting in an increased electric dipole transition matrix element [37]. Our results regarding structural, morphological and optical characterizations are in good agreement with those previously reported for rf-sputtered ZnSe thin films in the literature [28, 29].

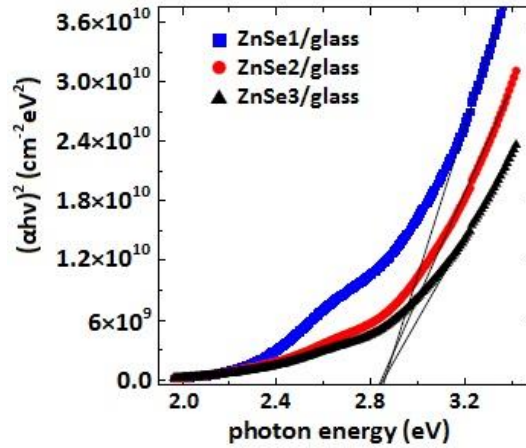


Fig. 4 – Dependence of optical absorption coefficient on the energy of the photons, as described by eq. (3), near the fundamental absorption edge of ZnSe films deposited on optical glass substrates. ZnSe1, ZnSe2 and ZnSe3 indicate the films with 110 nm, 150 nm and 175 nm thickness, respectively.

Spectroscopic ellipsometry was employed to determine the optical constants (refractive index  $n$  and extinction coefficient  $k$ ) for ZnSe thin films deposited on glass. The ellipsometric ( $\Psi$ ,  $\Delta$ ) spectra were recorded in reflected light at an incident angle of  $70^\circ$ , with respect to film surfaces. An optical three layers model (upper rough layer/ZnSe layer/glass substrate) was used and the dispersion model chosen for fitting spectra was Adachi-New Forouhi (ANF) model [38]. Spectra of refractive indices and extinction coefficients of the films are plotted in Fig. 5. One can observe that the refractive index tends to increase with increasing the thickness of the films. This may be explained by the quantum confinement effects associated to the small

size of the crystallites: there are larger crystallites in films with larger thickness (see Table 1). The decrease of the refractive index with the increase of photon wavelength in the visible region of the electromagnetic spectrum (VIS) indicates the normal dispersion behavior of ZnSe thin films in this region. In NIR region the refractive index tends to be relatively constant, the obtained values being in good agreement with previous works [39, 40]. Due to the fact that ZnSe films are almost transparent in NIR region, extinction coefficients were computed only for VIS region, their values increasing with photon energy. Increasing the thickness of ZnSe films leads to a decrease in extinction coefficients as shown in Fig. 5.

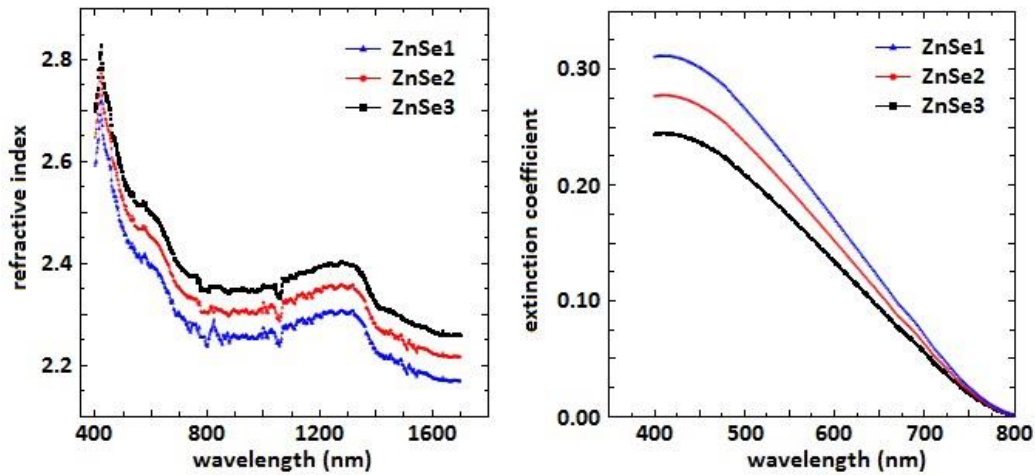


Fig. 5 – Wavelength dependence of the refractive index (left) and of the extinction coefficient (right) of ZnSe films deposited on optical glass substrates. ZnSe1, ZnSe2 and ZnSe3 indicate the films with 110 nm, 150 nm and 175 nm thickness, respectively.

The electrical resistivity of ZnSe films deposited on glass was investigated in a temperature range from 300 K to 10 K (Fig. 6). In the case of ZnSe, in the 300 K – 240 K temperature range, the dominant scattering mechanism of charge carriers is due to interaction of carriers with optical phonons, with an important polaron effect manifested in the renormalization of the carrier effective mass and in the peculiarities of the temperature dependence of the mobility [41, 42, 43, 44].

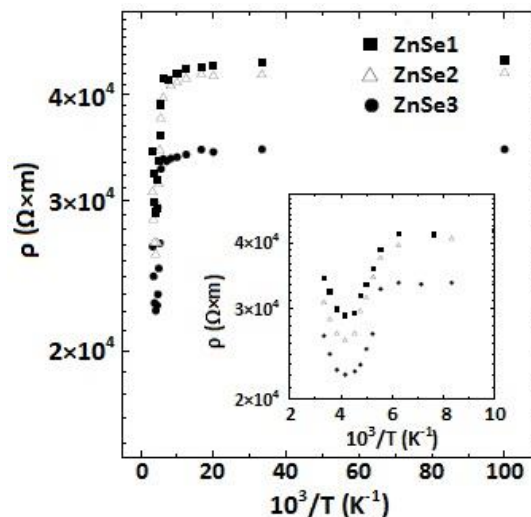


Fig. 6 – Arrhenius plot of the electrical resistivity of ZnSe films; a detailed view of the 300 K – 240 K range is shown in the inset. ZnSe1, ZnSe2 and ZnSe3 indicate the films with 110 nm, 150 nm and 175 nm thickness, respectively.

A further decrease of temperature leads to an increase of the resistivity, more pronounced in the range of 240 K – 100 K. This range corresponds to gradual freezing-out of conduction electrons, recaptured by donor centers, leading to an activated temperature dependence of the resistivity:

$$\rho = \rho_0 \exp\left(\frac{E_a}{k_B T}\right), \quad (4)$$

in which the activation energy  $E_a$  is the ionization energy of the main donors. Experimentally obtained values for the activation energy were 0.024 eV for 110 nm and 150 nm thick films, as well as 0.035 eV for 175 nm thick film. At lower temperatures the resistivity increases slightly with decreasing temperatures, due to a hopping mechanism. The resistivity values correlate well with the film thickness (thicker films are less resistive) and with the results of XRD investigations, showing that the crystalline disorder decreases with increasing thickness.

### 3.2. ZnSe/CdTe structures

ITO/ZnSe/CdTe/Cu:Au structures fabricated as explained in Section 2 were irradiated with protons (energy 3 MeV, fluence  $10^{13} \text{ cm}^{-2}$ ) and their electric and photovoltaic characteristics were investigated before and after irradiation.  $I$ - $V$  characteristics before and after irradiation, shown in Fig. 7 for the structure with a 150 nm thick ZnSe layer, are nonlinear and asymmetrical, being well described by the modified Shockley equation:

$$I = I_0 \left[ \exp\left(\frac{V - r_s I}{nk_B T}\right) - 1 \right] + \frac{V - r_s I}{R_{sh}}, \quad (5)$$

in which  $n$  is the effective quality factor of the structure,  $I_0$  is the reverse bias saturation current,  $r_s$  is the series resistance of the structure and  $R_{sh}$  is the shunt resistance. To characterize the effect of irradiation, experimental  $I$ - $V$  characteristics were fitted with equation (5) and the obtained values of the parameters were collected in Table 3.

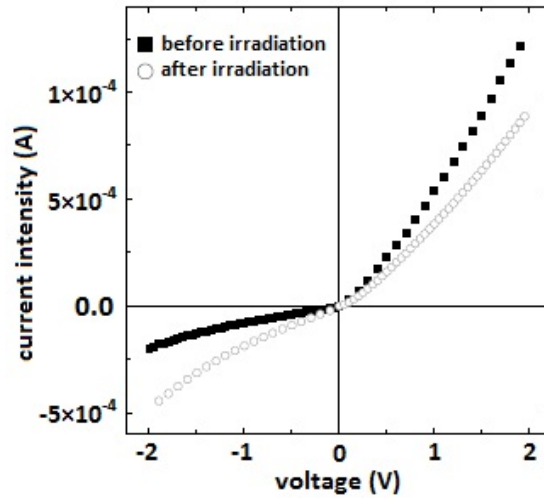


Fig. 7 – Dark  $I$ - $V$  characteristics of the structure ITO/ZnSe/CdTe/Cu:Au, before and after irradiation with protons (3 MeV, fluence  $10^{13} \text{ cm}^{-2}$ ). The thickness of ZnSe layer was 150 nm.

Table 3

Parameters of dark  $I$ - $V$  characteristics of ITO/ZnSe/CdTe/Cu:Au structure with 150 nm thick ZnSe layer

$I_0$ (A)	$n$	$r_s$ ( $\Omega$ )	$R_{sh}$ ( $\Omega$ )	Obs.
$1.1 \times 10^{-4}$	10.8	950	$9.32 \times 10^4$	before irradiation
$7.2 \times 10^{-5}$	14.8	1208	$1.07 \times 10^4$	after irradiation

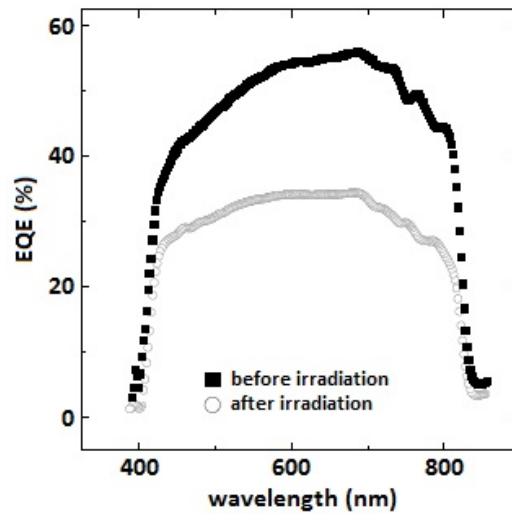


Fig. 8 – EQE action spectra of a ITO/ZnSe/CdTe/Cu:Au structure, before and after irradiation with protons (3 MeV, fluence  $10^{13} \text{ cm}^{-2}$ ). The thickness of ZnSe layer was 150 nm.

The asymmetry of  $I$ - $V$  characteristics is reduced after irradiation with protons, which leads to an increased value of the quality factor  $n$ . This can be explained by the increase of the recombination rate of photogenerated charge carriers in the space charge region, due to an increased density of recombination centers associated with structural defects induced by proton irradiation. Decreasing of reverse saturation current is due to the decrease in carriers' mobility.

Action spectra of the external quantum efficiency (EQE) of the ITO/ZnSe/CdTe/Cu:Au structure are shown in Fig. 8, before and after irradiation with protons. EQE, which measures the number of charge carriers collected at electrodes for an absorbed photon of a given energy, has a window of spectral response extending from 850 nm to 390 nm. The spectral range 800 nm – 600 nm corresponds to charge carriers photogenerated in CdTe absorber layer, while the range 600 nm – 450 nm corresponds to carriers' photogenerated in ZnSe window layer, proving that the space charge region extends in both layers of the structure. EQE is severely reduced after irradiation with protons, due to the recombination centers related to the structural defects introduced in the vicinity of ZnSe/CdTe interfaces.

#### 4. CONCLUSIONS

Highly textured polycrystalline ZnSe thin films were deposited on glass substrates and ITO covered glass substrates by rf-magnetron sputtering. It was found that, for the deposition conditions described here, the size of the crystallites tends to increase with increasing film thickness. The results of ellipsometric measurements have shown that the refractive index of the films increases also with the increase of thickness, which is attributed to the increase in particle size. There is a dip in the temperature dependence of the electrical resistivity, associated with a change in the transport mechanism, which at temperatures above 240 K corresponds to scattering of conduction band electrons by optical phonons in the saturation range (all donors are ionized), while in the range 240 K – 100 K the activated temperature dependence of the resistivity is due to the freezing-out of conduction band electrons, recaptured by donors. At temperatures below 100 K the charge transport mechanism is due to electrons hopping between localized states. ZnSe films were used as window layers in CdTe based photovoltaic structures fabricated in superstrate configuration. After irradiation with protons (3 MeV, fluence  $10^{13} \text{ cm}^{-2}$ ), although the parameters corresponding to dark  $I$ - $V$  characteristics are not significantly changed, the photovoltaic response is strongly altered. This is due to capture centers associated with structural defects introduced by proton irradiation in the space charge regions of the structure.

## ACKNOWLEDGEMENTS

The authors thank Dr. M.M. Gugiu (“Horia Hulubei” National Institute for R&D in Physics and Nuclear Engineering, Bucharest) for performing proton irradiations. Support from Romanian Executive Agency for Higher Education, Research, Development and Innovation (UEFISCDI) through the grants: 18PCCDI/2018; PN-III-P1-1.1-TE-2019-0868 (115/2020) and PN-III-P1-1.1-TE-2019-0846 (25/2020) is acknowledged.

## REFERENCES

1. M. GODLEWSKI, E. GUZIEWICZ, K. KOPALCO, E. LUSAKOWSKA, E. DYNOWSKA, M.M. GODLEWSKI, E.M. GOLDYS, M.R. PHILLIPS, *Origin of white color light emission in ALE-grown ZnSe*, J Lumin, **102**, pp. 455-459, 2003.
2. W.R. CHEN, C.J. HUANG, *ZnSe-based mixed-color LEDs*, IEEE Photonic Tech L, **16**, 5, pp. 1259-1261, 2004.
3. S. ARMSTRONG, P.K. DATTA, R.W. MILES, *Properties of zinc sulfur selenide deposited using a close-spaced sublimation method*, Thin Solid Films, **403**, pp. 126-129, 2002.
4. M. PRABHU, K. KAMALAKKANNAN, N. SOUNDARARAJAN, K. RAMACHANDRAN, *Fabrication and characterization of ZnSe thin films based low-cost dye sensitized solar cells*, J Mater Sci Mater Electron, **26**, 6, pp. 3963-3969, 2015.
5. P. XIN, J. LARSEN, F. DENG, W. SHAFARMAN, *Development of Cu(In, Ga)Se<sub>2</sub> superstrate device with alternative buffer layers*, Sol Energy Mater Sol Cells, **157**, pp. 85-92, 2016.
6. A. RUMBERG, C. SOMMERHALTER, M. TOPLAK, A. JAGER-WALDAU, M.C. LUX-STEINER, *ZnSe thin films grown by chemical vapour deposition for application as buffer layer in CIGSS solar cells*, Thin Solid Films, **361**, pp. 172-176, 2000.
7. B. ULLRICH, *Comparison of the photocurrent of ZnSe/InSe/Si and ZnSe/Si heterojunctions*, Mater Sci Eng B Solid State Mater Adv Technol, **56**, 1, pp. 69-71, 1998.
8. M.-Y. CHIU, C.-C. CHEN, J.-T. SHEU, K.-H. WEI, *An optical programming/electrical erasing memory device: Organic thin film transistors incorporating core/shell CdSe/ZnSe quantum dots and poly(3-hexylthiophene)*, Org Electron, **10**, 5, pp. 769-774, 2009.
9. L. YAN, J. WOOLLAM, E. FRANKE, *Oxygen plasma effects on optical properties of ZnSe films*, J Vac Sci Technol, **20**, 3, pp. 693-701, 2002.
10. T. L. CHU, S.S. CHU, G. CHEN, J. BRITT, C. FERKIDES, C.Q. WU, *Zinc selenide films and heterojunctions*, J Appl Phys, **71**, 8, pp. 3865-3869, 1992.
11. S. BANERJEE, R. PAL, A. MAITY, S. CHAUDHURI, A. PAL, *Nanocrystalline ZnSe films prepared by high pressure magnetron sputtering*, Nanostruct Mater, **8**, 3, pp. 301-312, 1997.
12. V. KUMAR, K. KHAN, G. SINGH, T. SHARMA, M. HUSSAIN, *ZnSe sintered films: Growth and characterization*, Appl Surf Sci, **253**, 7, pp. 3543-3546, 2007.
13. Q. ZHANG, H. LI, Y. MA, T. ZHAI, *ZnSe nanostructures: Synthesis, properties and applications*, Prog Mater Sci, **83**, pp. 472-535, 2016.
14. A. TERAN, C. CHEN, E. LOPEZ, P. LINARES, I. ARTACHO, A. MARTI, A. LUQUE, J. PHILLIPS, *Heterojunction band offset limitations on open-circuit voltage in p-ZnTe/n-ZnSe solar cells*, IEEE J Photovolt, **5**, 3, 874-877, 2015.
15. P. PRABUKANTHAN, G. HARICHANDRAN, *Electrochemical deposition of n-type ZnSe thin film buffer layer for solar cells*, J Electrochem Soc, **161**, 14, pp. 736-741, 2014.
16. A. KHURRAM, M. IMRAN, N. KHAN, M. MEHMOOD, *ZnSe/ITO thin films: candidate for CdTe solar cell window layer*, J Semicond, **38**, 9, p. 093001, 2017.
17. C. LOKHANDE, P. PATIL, H. TRIBUTSCH, A. ENNAOUI, *ZnSe thin films by chemical bath deposition method*, Sol Energy Mater Sol Cells, **55**, 4, pp. 379-393, 1998.
18. P.K. NAIR, M.T.S. NAIR, V.M. GARCIA, O.L. ARENAS, Y. PENA, A. CASTILLO, I.T. AYALA, O. GOMEZDAZA, A. SANCHEZ, J. CAMPOS, H. HU, R. SUAREZ, M.E. RINCON, *Semiconductor thin films by chemical bath deposition for solar energy related applications*, Sol Energy Mater Sol Cells, **52**, 3-4, pp. 313-344, 1998.
19. A. ENNAOUI, U. BLIESKE, M.C. LUX-STEINER, *13.7%-efficient Zn(S, OH)<sub>2</sub>/Cu(In, Ga)(S, Se)<sub>2</sub> thin-film solar cell*, Prog Photovoltaics, **6**, 6, pp. 447-451, 1998.
20. S. ANTOHE, L. ION, M. GIRTAN, O. TOMA, *Optical and morphological studies of thermally vacuum evaporated ZnSe thin films*, Rom Rep Phys, **65**, 3, pp. 805-811, 2013.
21. A. KHURRAM, F. JABAR, M. MUMTAZ, N. KHAN, M. MEHMOOD, *Effect of light, medium and heavy ion irradiations on the structural and electrical properties of ZnSe thin films*, Nucl Instrum Methods Phys Res B, **313**, pp. 40-44, 2013.
22. E. BACAKSIZ, S. AKSU, I. POLAT, S. YLMAZ, M. ALTUNBAS, *The influence of substrate temperature on the morphology, optical and electrical properties of thermal-evaporated ZnSe thin films*, J Alloys Compd, **487**, 1-2, pp. 280-285, 2009.
23. T. KIM, M. JUNG, D. LEE, E. OH, S. LEE, H. JUNG, M. KIM, J. KIM, H. PARK, J. LEE, *Structural and optical properties of undoped and doped ZnSe/GaAs strained heterostructures*, Thin Solid Films, **298**, 1-2, pp. 187-190, 1997.
24. G. RIVEROS, H. GOMEZ, R. HENRIQUEZ, R. SCHREBLER, R. MAROTTI, E. DALCHIELE, *Electrodeposition and characterization of ZnSe thin films*, Sol Energy Mater Sol Cells, **70**, 3, pp. 255-268, 2001.
25. O. TOMA, L. ION, S. IFTIMIE, A. RADU, S. ANTOHE, *Structural, morphological and optical properties of rf-sputtered CdS thin films*, Mater Des, **100**, pp. 198-203, 2016.

26. H. YUDAR, S. PAT, S. KORKMAZ, S. OZEN, V. SENAY, *Zn/ZnSe thin films deposition by RF magnetron sputtering*, J Mater Sci, **28**, 3, pp. 2833-2837, 2017.
27. O. TOMA, L. ION, S. IFTIMIE, V.A. ANTOHE, A. RADU, A.M. RADUTA, D. MANICA, S. ANTOHE, *Physical properties of rf-sputtered ZnS and ZnSe thin films used for double-heterojunction ZnS/ZnSe/CdTe photovoltaic structures*, Appl Surf Sci, **478**, pp. 831-839, 2019.
28. M.A. SAYEED, H.K. ROUF, K.M.A. HUSSAIN, *Effect of thickness on characteristics of ZnSe thin film synthesized by vacuum thermal evaporation*, J Theor Appl Phys, **14**, pp. 251-259, 2020.
29. M.F. HASANEEN, Z.A. ALROWAILI, W.S. MOHAMED, *Structure and optical properties of polycrystalline ZnSe thin films: validity of Swanepol's approach for calculating the optical parameters*, Mater Res Express, **7**, p. 016422, 2020.
30. O. TOMA, L. ION, M. GIRTAN, S. ANTOHE, *Optical, morphological and electrical studies of thermally vacuum evaporated CdTe thin films for photovoltaic applications*, Sol Energy, **108**, pp. 51-60, 2014.
31. A.R. FLORES, R. CASTRO-RODRIGUEZ, J.L. PENA, N. ROMEO, A. BOSIO, *Characterization of CdTe films with in situ CdCl<sub>2</sub> treatment grown by a simple vapor phase deposition technique*, Appl Surf Sci, **255**, 15, pp. 7012-7016, 2009.
32. S. LALITHA, R. SATHYAMOORTHY, S. SENTHILARASU, A. SUBBARAYAN, *Influence of CdCl<sub>2</sub> treatment on structural and optical properties of vacuum evaporated CdTe thin films*, Sol Energy Mater Sol Cells, **90**, 6, pp. 694-703, 2006.
33. O. TOMA, S. IFTIMIE, C. BESLEAGA, T. MITRAN, V. GHENESCU, O. PORUMB, A. TODERAS, M. RADU, L. ION, S. ANTOHE, *New investigations applied on cadmium sulfide thin films for photovoltaic applications*, Chalcogenide Lett, **8**, 12, pp. 747-756, 2011.
34. I. BURDUCEA, M. STRATICIUC, D.G. GHITA, D.V. MOSU, C.I. CALINESCU, N.C. PODARU, D.J.W. MOUS, I. URSU, N.V. ZAMFIR, *A new ion beam facility based on a 3 MV Tandetron™ at IFIN-HH, Romania*, Nucl Instrum Methods Phys Res B, **359**, pp. 12-19, 2015.
35. K. WRIGHT, G. WATSON, S. PARKER, D. VAUGHAN, *Simulation of the structure and stability of sphalerite (ZnS) surfaces*, Am Mineral, **83**, 1-2, pp. 141-146, 1998.
36. J.I. LANGFORD, R. DELHEZ, T.H. KEIJSER, E.J. MITTEMEIJER, *Profile analysis for microcrystalline properties by the Fourier and other methods*, Aust J Phys, **41**, 2, pp. 173-188, 1988.
37. A.D. YOFFE, *Semiconductor quantum dots and related systems: electronic, optical, luminescence and related properties of low dimensional systems*, Adv Phys, **50**, 1, pp. 1-208, 2001.
38. H. YOSHIKAWA, S. ADACHI, *Optical constants of ZnO*, Jpn J Appl Phys Pt 1, **36**, 10, pp. 6237-6243, 1997.
39. M. ASHRAF, S.M.J. AKHTAR, A.F. KHAN, Z. ALI, A. QAYYUM, *Effect of annealing on structural and optoelectronic properties of nanostructured ZnSe thin films*, J Alloys Compd, **509**, 5, pp. 2414-2419, 2011.
40. Y.P.V. SUBBAIAH, P. PRATHAP, M. DEVIKA, K.T.R. REDDY, *Close-spaced evaporated ZnSe films: preparation and characterization*, Physica B, **365**, 1-4, pp. 240-246, 2005.
41. O.V. EMELYANENKO, G.N. IVANOVA, T.S. LAGUNOVA, D.D. NEDEOGLO, G.M. SHMELEV, A.V. SIMASHKEVICH, *Scattering mechanisms of electrons in ZnSe crystals with high mobility*, Phys Status Solidi B Basic Res, **96**, 2, pp. 823-833, 1979.
42. S. ANTOHE, L. ION, V.A. ANTOHE, *The effect of the electron irradiation on the structural and electrical properties of A(II)-B-VI thin polycrystalline films*, Journal of Optoelectronics and Advanced Materials, **5**, 4, pp. 801-816, 2003.
43. G. SOCOL, D. CRACIUN, I. N. MIHAILESCU, N. STEFAN, C. BESLEAGA, L. ION, S. ANTOHE, K. W. KIM, D. NORTON, S. J. PEARTON, A. C. GALCA, V. CRACIUN, *High quality amorphous indium zinc oxide thin films synthesized by pulsed laser deposition*, Thin Solid Films, **520**, 4, pp.1274-1277, 2011.
44. I. VAICIULIS, M. GIRTAN, A. STANCULESCU, L. LEONTIE, F. HABELHAMES, S. ANTOHE, *On titanium oxide spray deposited thin films for solar cells applications*, Proceedings of the Romanian Academy, Series A: Mathematics, Physics, Technical Sciences, Information Science, **13**, 4, pp. 335-342, 2012.

Received February 19, 2021